Journal Name

ARTICLE

Received 00th January 20xx,
Accepted 00th January 20xx
DOI: 10.1039/x0xx00000x
www.rsc.org/

# A Polybenzimidazole/Graphite Oxide based three layer membranes for intermediate temperature polymer electrolyte membrane fuel cells

Yuming Deng[a, b], Gang Wang[c], MingMing Fei[a,b], Xin Huang[a], Jigui Cheng[a], Xiaoteng Liu[d], Lei Xing[e], Keith Scott[f], Chenxi Xu[*, a]

A three layer membrane (TLM) of Polybenzimidazole/Graphite Oxide/Polybenzimidazole (PBI/GO/PBI) has been fabricated as an electrolyte for intermediate temperature polymer exchange membrane fuel cells (IT-PEMFCs). The membrane is prepared by encapsulating a GO layer with two single PBI membranes via a layer-by-layer procedure and subsequently imbibed with phosphoric acid (PA). The TLM exhibits a lower swelling ratio than that of the pristine PBI membrane at the same PA loading time. The mechanical strength of the TLM could reach 28.6MPa at 150℃, significantly higher than that of a PBI membrane (12.2MPa). The TLM is loaded with a PA amount of 2.23 H3PO4 molecules per repeat unit (PRU), which provides a proton conductivity of 0.0138 S $cm^{-1}$ at 150℃. Three layers structure promotes membrane for PEMFCs with lower PA leakage and material corrosion. The fuel cell performance based on TLM exhibits a peak power density of 210 $mWcm^{-2}$ at 150℃.

## Introduction

Proton exchange membrane fuel cells (PEMFCs) have been considered as next generation power sources due to their many benefits, such as environment friendly, safety, low noise, rapid start, high efficiency and power density [1-5]. The electrolyte membrane is a key part of the PEMFC, and the most investigated electrolyte materials are perfluorosulfonic acid membranes such as Nafion© which has been a reference material within the market [6-10]. Yong et al. used a Nafion/graphite oxide composite as an electrolyte membrane and achieved a power density of 841 mW $cm^{-2}$ at 80℃ [11]. Recently, considerable efforts have been made to develop higher temperature (>100℃) PEMFCs using polymer acid complexes (PACs) because they offer significant advantages in this temperature range, such as (1) improved CO tolerance, (2) enhanced efficiency, (3) avoidance of flooding by water, (4) opportunity to use non-noble metal catalysts, and (5) system simplification[12-18]. The phosphoric-acid (PA) loaded polybenzimidazole (PBI) is the best-known example of a membrane for HT-PEMFC. Li et al. achieved a power density of 550 mW $cm^{-2}$ at 190℃ and at atmospheric pressure with PBI/PA membranes [19]. Pinar et al used PBI membrane with Titanium and other composite as electrolyte membrane achieved a serious of high power density and well electrochemical stability [20-24]. However, in many cases, PBI/PA membranes only exhibit high conductivity with high acid loadings, usually at least higher than 5.0 $H_3PO_4$ molecules per repeat unit (PRU) of PBI. Such a high PA acid content causes problems of mechanical strength reduction and elution of acid electrolyte, as well as catalyst corrosion, especially at high temperature [25]. Also, a high swelling of the membrane leads to a wrinkling of the filmwhich can reduce the contact area between the membrane and electrode.

[a] School of Materials Science and Engineering, Hefei University of Technology, Hefei, Anhui, China, 230009
[b] Institute of industry & Equipment technology, Hefei University of Technology, Hefei, Anhui, China, 230009
[c] I China quality certification centre, Beijing, China, 100070
[d] Department of Mechanical & Construction Engineering, Faculty of Engineering and Environment, Northumbria University, UK, NE1 8ST
[e] Institute of Green Chemistry and Chemical Technology, Jiangsu University, Zhenjiang, China, 212013
[f] School of Chemical Engineering and Advanced Materials, Newcastle University, Newcastle NE1 7RU, United Kingdom
* Corresponding Author, E-mail: xuchenxi31@126.com

One promising idea to reduce the PA loading is to utilise a layer of solid proton conductors, which is less expandable, between the PBI membranes. One such material is graphite oxide (GO) [26-29]. Graphite Oxide with its many hydroxyl and carboxyl groups can form hydrogen bonds with $H_3PO_4$ and $H_2O$ that benefit proton conductivity [30]. Our previous work with PBI/GO composite membranes, with 2 PRU PA, in IT-PEMFC produced a power density of 380 $mWcm^{-2}$ [31]. GO also has a lower PA absorption and is less expandable, which may help to decrease the swelling of the membrane. Also the interaction between the GO layer and polymer matrix may increase the mechanical strength of the composite electrolyte [32]. So, a single GO layer centrally located in the membrane may be a way to improve the mechanical strength and reduce the PA doping level whilst retaining good proton conductivity. In this work, three layers membrane (PBI/GO/PBI) was prepared for a HT-PEMFC, and the swelling ratio, proton conductivity and fuel cell performance of the membrane were studied.

## Experimental

### Chemicals and reagents

Expandable graphite power was purchased from Shandong Qingdao graphite (China), Phosphoric acid (85 wt%), dimethylacetamide (DMAc), hydrogen peroxide (5%), potassium permanganate, hydrochloric acid and sulfuric acid were purchased from Sinopharm Chemical Reagent Co. Ltd (China). PBI powder was purchased from Caleed Between inc. PBI powder (intrinsic viscosity IV=0.7-0.9 dl/g).

### Graphite oxide (GO) Preparation

Graphite oxide was prepared according to the modified Hummers method as shown in scheme 1 [33-35]. Briefly, 360 $cm^3$ (ml) sulfuric acid and 40 ml phosphoric acid solution was vigorously stirred in s three-neck flask and then the graphite powder and potassium permanganate were added. The mixture was heated at 50℃ for 12h, and then poured into a solution of 20 ml hydrogen peroxide and 500ml deionized water. The mixture was then rinsed with hydrochloric acid and deionized water several times.

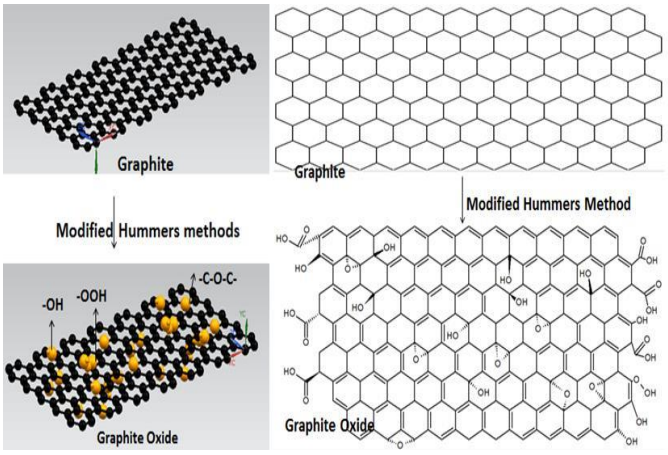


Scheme1, Schematic of graphite oxide (GO) structure

### PBI-GO-PBI membrane Preparation

A 5 wt% PBI solution was prepared from 2g poly (2, 2'-m-(phenylene)-5, 5'-bibenzimidazole) (PBI) powder dissolved in 50ml dimethylacetamide (DMAc). 0.1g GO powder was added into 1g 5 wt. % PBI solution with ultrasonic mixing. 4ml PBI/DMAc solution were poured onto a film casting machine, and dried at 60 ºC for 2hrs. The PBI/GO solution was poured on the PBI layer and dried at 60 ºC for 1 hour. Finally, another 4ml PBI solution was poured on PBI/GO layer to prepare the TLM as shown in scheme 2.

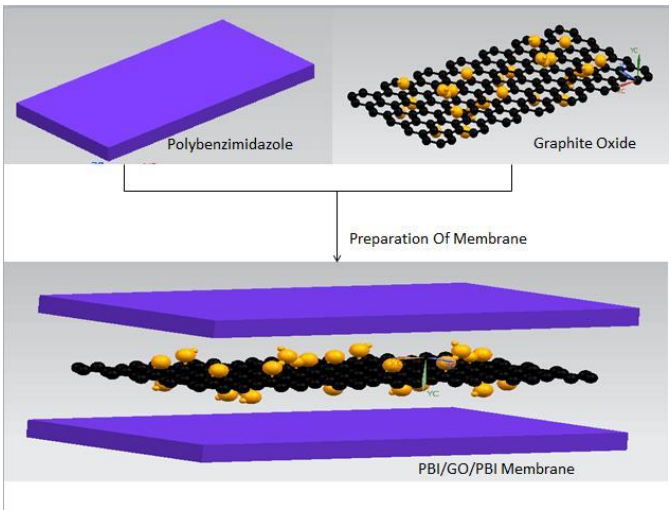


Scheme 2, Schematic of PBI/GO/PBI membrane preparation

### Characterizations of PBI membrane and PBI/GO/PBI membrane

The crystal structures of different membranes were analysed by X-ray diffraction (XRD) using a PANalytical X ' Pert Pro Diffractometer, with a 2θ

range of 5-40°. The membrane morophologies were measured by a JSM-5300LV (Japan) Scanning Electron Microscope (SEM).

Tensile measurements were performed on samples of membrane 25mm in length and 1mm wide, with a thermal mechanical analyzer (NETZSCH TMA402F3) at 150℃ at a speed of 0.2 mm/min. The tensile strength and elongation at break point were recorded to evaluate the mechanical properties of the membranes. The value was calculated from the average of five times results.

**PA doping level and Volume swelling test**

PBI membrane and PBI/GO/PBI membrane was dried in a vacuum oven at 120℃ until no further weight loss. Then the two membranes were loaded with aqueous 3 mol $dm^{-3}$ (M) PA for 20h. The PA loading (doping level (DL)) [36] was calculated from the membrane weight gain using Eq. (1)

$$\text{PA doping level} = \frac{(w_2 - w_1) \times M_{membrane}}{w_1 \times M_{H_3PO_4}} \quad (1)$$

Where $W_2$ is the weight of acid loaded membrane and $W_1$ is the dry membrane weight which was dried in a vacuum oven at 120℃ until no further weight loss. $M_{membrane}$ is the relative molecular mass of the membrane and $M_{H3PO4}$ is the relative molecular mass of the $H_3PO_4$.

The volume swelling ratio is defined as the percentage of the membrane volume increase after PA treatment and is determined by Eq. (2) [36].

$$\text{Swelling ratio}(\%) = \frac{V_1 - V_0}{V_0} \times 100 \quad (2)$$

Where $V_1$ and $V_0$ are volumes of membrane after and before PA doping

**Leaching Test**

The leaching test were carried out by washing the doped membranes in water at 50℃-90℃ for 2hrs [37]. The phosphoric acid removed from the membrane was measured by Eq. (3).

$$\text{Remaining acid} = \frac{(w_2^{a,b,c} - w_1) \times M_{membrane}}{w_1 \times M_{H_3PO_4}} \quad (3)$$

Where $W_2^a$, $W_2^b$ and $W_2^c$ are the weight of acid loaded membrane after washing the doped membranes in water at 25 ºC , 50ºC and 80 ºC for 2 hrs, respectively. $W_1$ is the dry membrane weight which was dried in a vacuum oven at 120℃ until no further weight loss.

**Proton Conductivity Test**

The proton conductivity of the composite membranes was measured using a four-point probe method, under non-humidified conditions at atmospheric pressure (with an Autolab PGSTAT302) using AC impedance measurements carried out between frequencies of 1 to $10^6$ Hz and with an applied voltage of 10 mV [38]. To ensure the membrane reached a steady state, the membranes were held at the desired conditions for 2 hours before testing, and measurements were taken at 30 min intervals. The proton conductivity was determined by Eq. (4).

$$\delta = \frac{L}{twR} \quad (4)$$

Where L is the length between the two electrodes, t and w are the thickness and width of the membrane. R is the resistance of the membrane.

**Fuel Cell Performance**

Catalyst inks were prepared by blending carbon supported catalysts (40 wt. % Pt/C, Alfa Aesar) in a water-ethanol mixture under ultrasonic vibration for 10 min. Gas diffusion electrodes (carbon paper, H2315T10AC1 from Freudenburg Germany) incorporated with wet proofed micro-porous layer was used as substrates to deposit the catalyst layer for both the anode and the cathode. The catalyst inks were sprayed onto carbon substrates at 100 ºC, and the electrodes were held at 150 ºC for 2 h to allow liquid to evaporate. The Pt loadings on both cathode and anode were 0.6 mg $cm^{-2}$. The membrane electrode assemblies （MEA) was finally obtained by hot pressing the electrodes onto phosphoric acid loaded composite membranes at 150 ºC for 10 min with a load of 40 kg $cm^{-2}$. The MEA was fixed between two high-density graphite blocks (impregnated with phenolic resin) with parallel gas flow channels, and the active electrode area was 1 $cm^2$. Electric cartridge heaters were mounted at the rear of the graphite blocks to maintain the desired temperature, which was monitored using imbedded thermocouples and controlled with a temperature controller. $H_2$ and $O_2$ were fed into the cell at flow rates of 100 $cm^3$ $min^{-1}$ and atmospheric pressure [39]. To ensure the fuel

cell performance reached a steady state, the cell were held at 100 °C for 6 hrs and then elevated to each desired conditions for 6hrs before performing the measurements. The stability test was used a PBI/GO/PBI membrane that operated 150℃ without any humidification of $H_2$ and $O_2$ . The applied current density was 0.2 A $cm^{-2}$ for 72 hrs [33].

## Results and Discussion

### Characterization of GO and PBI/GO/PBI membrane

Expandable graphite was oxidized by sulfuric acid and potassium permanganate with incorporation of functional groups into their galleries, including hydroxyl carboxyl, phenol groups and oxygen epoxide groups [40]. XRD data for the material is shown in Fig. 1. The typical graphite diffraction peak (002) normally exhibits at 2θ = 26.4° and the interlayer space is 0.34 nm. The X-ray diffraction pattern of graphite oxide (GO) exhibited a corresponding reflection peak at 9.5° with an inter layer spacing of 0.93 nm. The planar distance increase of GO comes from the existence of functional groups, which indicates that the oxidation of graphite was successful. The diffraction peak of PBI/GO/PBI is at 8.3° with an interlayer spacing of 1.04 nm, and this higher layer distance may be attributed to the introduction PBI into GO layers.

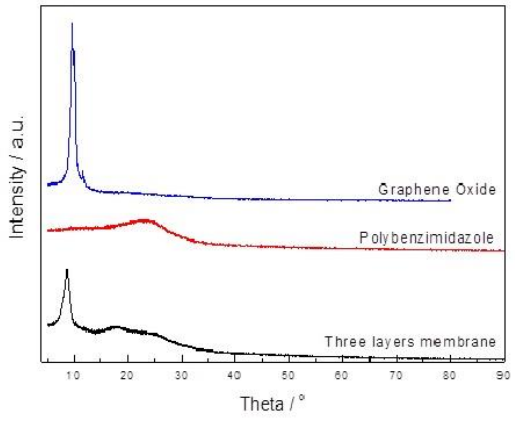


Figure1, XRD spectra of GO, PBI, PBI/GO/PBI membranes

SEM data for the GO showed a typical lamellar structure of GO as depicted in Fig.2 (a), indicating that a layer structure of GO was produced by the synthesis method. Figure 2 (b) shows the SEM for the PBI/GO/PBI three layer membrane (TLM) where the central lamellar part is the GO layer and the smooth outer parts is PBI. The GO sheet remained exfoliated in the and tightly immobilized in the PBI matrix, according to the strong interfacial interactions. Therefore, conduction paths have been established through the entire ILM, and these conduction paths will provide a possible route to provide good proton conductivity.

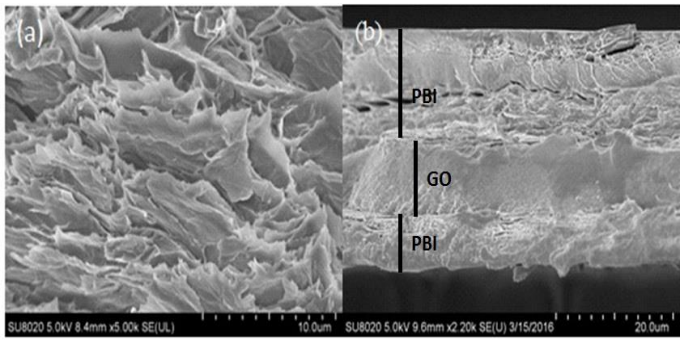


Figure 2, SEM images of membrane cross-sections: (a) GO, (b) PBI/GO/PBI

### PA uptake, swelling ratio and mechanical properties of PBI and PBI/GO/PBI membrane

The variation in PA loading and swelling ratio with time of TLM and PBI membranes when immersed in 3M phosphoric acid are shown in Fig. 3 and Fig. 4 respectively. Both the PA loading and the swelling ratio increased with the time. However, after 35h doping, the doping level reached a peak value, and the curve of swelling ratio trends flat, indicating that a balance of PA acid between the internal and external of membrane is achieved. At 48h, the PA loading and swelling ratio of PBI were

3.05 PRU and 17.6% respectively whilst those of the TLM were 2.23 PRU and 9.35%, respectively. The GO structure has thus hindered the acid uptake, and also the bond interaction between GO and PBI will reduce the expansion. GO with lower expandable capability with acid will reduce the membrane fold and benefit the membrane assembly.

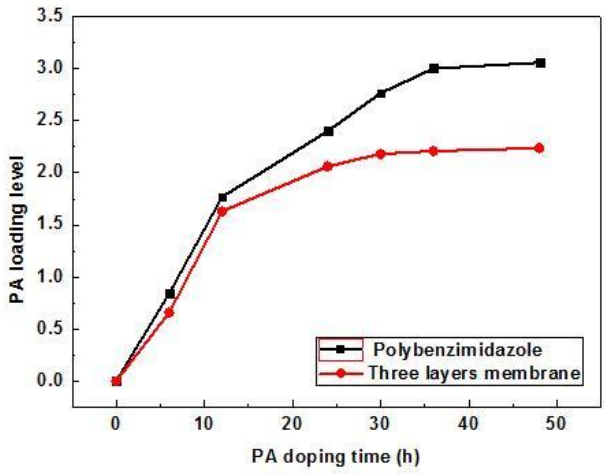


Figure3, Variation of PA loading level for PBI membrane and PBI/GO/PBI membrane

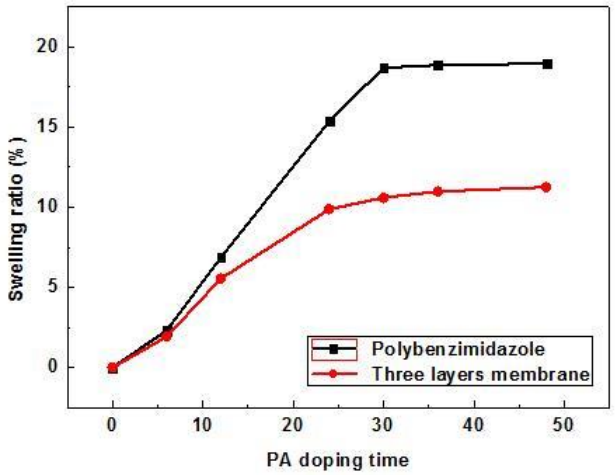


Figure 4, The swelling ratio of PBI/GO/PBI membrane and PBI membrane versus PA doping level increasing

As shown in table 1, the mechanical strength of PBI/PA and TLM/PA were 12.21MPa and 28.6 MPa at 150oC, with 3.05 and 2.23 PRU, respectively. The elongation at break of TLM was 9% and 26% of PBI membrane, indicating a higher strength of TLM.

This result may be caused by a lower swelling ratio of TLM and a higher interaction force between GO and PBI. The GO layer exhibits a lower expansion and higher mechanical performance under PA acid loading, indicating a potential longer lifetime when used in fuel cell applications.

Table 1, Mechanical properties of PBI (PRU 3.05) and PBI/GO/PBI (PRU 2.23) at 150℃

| Samples | Thickness | Tensile strength | Elongation |
|---|---|---|---|
| PBI | 33.6μm | 12.2MPa | 17.6% |
| TLM | 74μm | 28.6MPa | 9.35% |

The PA content retained in the membranes after leaching test at various temperatures was depicted in table 2. The PA content was reduced with the temperature increasing due to the water and acid leaching faster. The remained content of TLM was lower than that of PBI at 20℃ and 50℃according to the acid mainly absorbed by the PBI membrane rather than GO. However, the situation changed to the opposite up to 80℃. Because the acid amount was low enough that the weight loss is mainly caused by the water and GO had much better water remain capability.

**Table 2,** Phosphoric acid retained in the membranes after leaching test at 20℃, 50℃ and 80℃

| Temperature | PBI | PBI/GO/PBI |
|---|---|---|
| 25℃ | 3.1 | 2.3 |
| 50℃ | 1.17 | 1.075 |
| 80℃ | 0.665 | 0.70 |

## Proton conductivity

As depicted in Fig.6, the TLM exhibited a higher conductivity of 0.0138 $Scm^{-1}$, (3.05

PRU) than the pristine PBI membrane 0.0078 $Scm^{-1}$ (at PRU 2.23). However, the conductivity decreased down when the temperature at higher temperature than 150 ℃. Water is an important role in improving the proton transfer mechanism. The conductivity decreased down is caused by the self-dehydration of $H_3PO_4$ and the loss of water when the temperature exceeds 150 ℃. [20]. Normally, a higher PA content in PBI provides higher proton conductivity, whereas in this case the TLM had a higher conductivity despite a lower PA loading. This result indicates that the GO layer in the polymer matrix is a suitable way to reduce the loading level of the membrane whilst achieving a similar conductivity with a PBI only membrane. The functional groups (carboxylic, hydroxyl and epoxy) of GO probably form hydrogen bonds with $H_2PO_4$ and $H_2O$ and provide more facile hopping of protons to enhance the conductivity. Thus overall the GO layer in TLM both enhanced the conductivity of membrane, and also improved the mechanical strength, making it suitable as a fuel cell membrane.

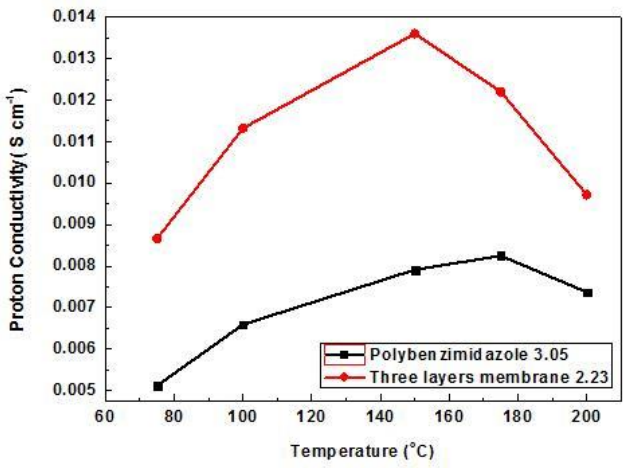


Figure 5, Variation of Proton conductivity of PBI and PBI/GO/PBI membranes with temperature

## Fuel cell performance

The polarization and power density curves of fuel cell with $H_2$ fuel and $O_2$ at 150℃ under anhydrous conditions at atmospheric pressure are shown in Fig.6. The open circuit voltages (OCV) of both PBI and TLM were higher than 0.85V. The performance of the cells with the TLM membranes was significantly better than that of the pristine PBI membrane at the similar PA loading. The performance was elevated with the temperature increasing, and the performance of TLM at 120℃ was also higher than that of PBI at 150℃, which is consistent with the conductivity results. The peak power densities of PBI and TLM were 160 mW $cm^{-2}$ and 210 $mWcm^{-2}$ at 150℃, respectively. The improved performance was mainly attributed to the superior proton conductivity of the latter membrane and also the strong acid and water retention properties of the composite membrane at low acid loading. Hydrogen bonds in GO, which form acidic functional groups, such as carboxylic acid, and epoxy oxygen group, could provide more facile hopping of protons to enhance the conductivity. And also the better mechanical strength and lower expansion after PA loading may also result in a structurally better membrane assembly which may be also result in better performance of the TLM.

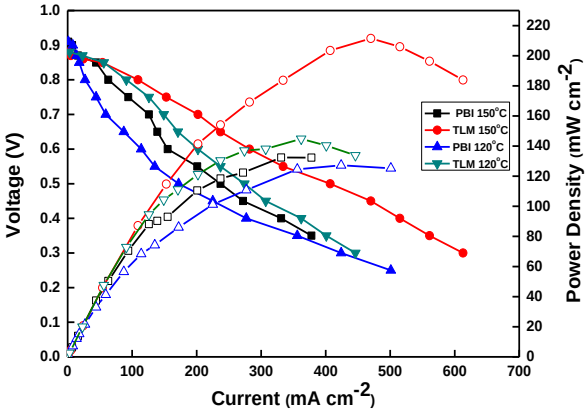


Figure 6, Polarization and power density curves of a fuel cell at 120℃ and 150℃ with $H_2/O_2$ atmospheric pressure and Pt loading: 0.6 mg $cm^{-2}$ both in cathode and anode

The internal resistance values were estimated from the current density change in the intermediate voltage losses range.

The current density change of the PBI and TLM based fuel cell were 177 mA $cm^{-2}$ and 227 mA $cm^{-2}$ (voltage from 0.35 V and 0.55 V), respectively, and resulted in cell conductivities of approximately 0.003 S $cm^{-1}$ and 0.0084 S $cm^{-1}$ of PBI and TLM, respectively.

This conductivity was much less than that of the membranes alone (approximately 50 % lower), which indicated a significant voltage loss in the electrode layers (and other cell components), i.e., the catalyst compositions in the MEA were not "optimal" for the fuel cell. Due to the low PA loading used in electrode, the electrode layer would have a relatively low ionic conductivity; thus, the catalyst utilization in the electrode reactions was low. Essentially, only the Pt particles adjacent to the membrane were active, consequently explaining, in part, the high electrode activation lost.

## Conclusions

A three layers PBI/GO/PBI composite electrolyte membrane has been successfully prepared for IT-PEMFC. The proton conductivity of 0.0138 $Scm^{-1}$ and a power density of 210 $mWcm^{-2}$ of TLM under $H_2/O_2$ condition at 150℃ are higher than that of pristine PBI membrane (0.0078 $Scm^{-1}$ and 160 $mWcm^{-2}$). The mechanical strength of the TLM (28.6 MPa) at 150℃ is nearly two times of the PBI membrane (12.2 MPa), and also a lower swelling ratio of TLM was obtained. The higher fuel cell performance of TLM loaded with low PA content is attributed to the higher conductivity and mechanical properties indicating that the PBI/GO/PBI composite membrane is a potential candidate as an electrolyte for intermediate temperature PEMFC. Further development of more active catalyst layers is required to improve fuel cell performance to levels which are commercially attractive.

## Acknowledgement

The authors thank the funding support provided by the Fundamental Research Funds for the Central Universities (2015HGCH001) and the Anhui Provincial Natural Science Foundation for the Returned Overseas Chinese Scholars, State Education Ministry (JZ2015JYLH0084) and the56th China Postdoctoral Science Foundation funded project (2014M560506).

## Notes and references

1 Q. Li, J. Jensen, F. Savinell, N. Bjerrum, J. Prog Polym Sci, 2009, 34, 449–477.
2 Q. Li, N. Bjerrum, J. Jensen, Fuel Cells, 2004, 4, 59-147.
3 W. Hogarth, J. Costa, M. Lu, J. Power Sources, 2005, 142, 223-229.
4 U. Beuscher, S. Cleghorn, W. Johnson, Int J. Energ Res, 2005, 29, 1102-1112.
5 T. Ratlamwala, E. Sinawi, M. Cadalla, A. Aidan, Int. J. Energ Res, 2012, 36, 1121-1132.
6 K. Mauritz, R. Moore, Chem Rev, 2004, 104, 4535–4586.
7 T. Zhu, Z. Yang, M. Han, Fuel, 2015, 161, 168-173.
8 Z. Liu, B. Ge, K. Li, X. Zhang, K. Huang, Fuel, 2016, 176, 173-180.
9 J. Varcoe, P. Atanassov, D. Dekel, A. Herring, Energy Environ Sci, 2014, 7, 3135-3191.
10 C. Laberty-Robert, K. Vallé, F. Pereira, C. Sanchez, Chem Soc Rev, 2011, 40, 961-1005.
11Y. Kim, K. Ketpang, S. Jariphun, J. Park, S. Shanmugam, J. Mater Chem A, 2015, 3, 8148-8155.
12 S. Thomas, A. Bates, S. Park, A. Sahu, Appl Energy, 2016, 165, 765-776.
13 K. Ahmed, K. Föger, Ind. Eng. Chem Res, 2010, 49, 7239-7256.
14 J. Gao, G. Wang, Z. Wang, Y. Wang, J. Liu, J. Membr Sci, 2014, 2, 19275-19281.
15 X. Huang, Y. Deng, C. Xu. L Yanga, Y. Hu, P. Luo, Y. Lu, J. Cheng, Fuel, 2016, 179, 299-304.
16 R. Devanathan, Energy Environ Sci, 2008, 1, 101–119.
17 D. Plackett, A. Siu, Q. Li, Q. Pan, J. Jensen, S. Nielsen, A. Anastasia, Fuel and Energ Abstr, 2011, 383, 78-87.
18 K. Scott, C. Xu, X. Wu, Wiley Interdisciplinary Reviews: Energy and Environment, 2014, 3, 24-41.
19 Q. Li, H. Hjuler, N. Bjerrum, J. Appl Electrochem, 2001, 31, 773-779.
20 F.J. Pinar, P. Canizares, M. Rodrigo, D. Ubeda, J. Lobato, RSC adv, 2012, 2, 1547-1556.

21 F.J.Pinar, P. Canizares, M. Rodrigo, D. Ubeda, J. Lobato, J. Power Source, 2011, 196, 4306-4313.
22 F.J.Pinar, P. Canizares, M. Rodrigo, D. Ubeda, J. Lobato, J. Power Source, 2015, 274, 177-185.
23 J. Lobato, P. Canizares, M. Rodrigo, D. Ubeda, F.J.Pinar, J. Power Source, 2011, 8265-8271.
24 J. Lobato, P. Canizares, M. Rodrigo, F.J.Pinar, D. Ubeda, J. Power Source, 2011, 4209-4217.
25 S.J. Peighambardoust, S. Rowshanzamir, M. Amjadi, Int J. Hydrog Energy, 2010, 35, 9349-9384.
26 W. Hogarth, J. Costa, G. Lu, J. Power Sources, 2005, 142, 223-231.
27 S. Jiang, J. Mater Chem A, 2014, 2, 7637-7655.
28 Y. Liu, W. Lehnert, H. Janßen, J. Power Sources, 2016, 311, 91-102.
30 S. Lu, R. Xiu, D. Liang, H. Wang, Y. Xiang, J. Membr Sci, 2014, 464, 1-7.
31 C. Xu, Y. Cao, R. Kumar, X. Wu, X. Wang, K. Scott, J. Mater Chem, 2011, 21, 11359-11364.
32 J. Linares, L. Battirola, J. Lobato, Springer, 2016, 13, 275-295.
33 C. Xu, X. Liu, J. Cheng, K. Scott, J Power Source, 274, 922-927.
34 N. Kovtyukhova, P. Olliver, B. Martin, T. Mallouk, T. Chizhik, S. Buzaneva, E. Gorchinskiy, Chem Mater, 1999, 11, 771-778.
35 D.C. Marcano, D. Kosynkin, D. Berlin, J. Sinitskii, Z. Sun, Z. Slesarev, L. Alemany, W. Lu, J. Tour, ACS Nano, 2010, 4, 4806-4814.
36 T. Zhou, R. Shao, S. Chen, X. He, J. Qiao, J. Power Sources, 2015, 293, 946-975.
37 F.J. Pinar, P. Can˜izares, M. A. Rodrigo, D. Ubeda, J. Lobato, RSC adv, 2012, 2, 1547-1556.
38 I. Hartung, S. Kirsch, P. Zihrul, O. Müller, T. Unwerth, J. Power Sources, 2016, 307, 280-288.
39 A. Iwan, M. Malinowski, G. Pasciak, Renew. Sust Energ Rev, 2015, 49, 954-967.
40 S. Sarkar, K. Raul, S. Pradhan, S. Basu, A. Nayak, Physica E, 2014, 64,78-82.